

PAPER • OPEN ACCESS

Roton in a few-body dipolar system

To cite this article: R Odziejewski *et al* 2018 *New J. Phys.* **20** 123006

View the [article online](#) for updates and enhancements.



IOP | ebooksTM

Bringing you innovative digital publishing with leading voices to create your essential collection of books in STEM research.

Start exploring the collection - download the first chapter of every title for free.



PAPER

Roton in a few-body dipolar system

OPEN ACCESS

RECEIVED

17 August 2018

REVISED

8 November 2018

ACCEPTED FOR PUBLICATION

21 November 2018

PUBLISHED

5 December 2018

Original content from this work may be used under the terms of the [Creative Commons Attribution 3.0 licence](#).

Any further distribution of this work must maintain attribution to the author(s) and the title of the work, journal citation and DOI.

R Ołdziejewski¹ , W Górecki, K Pawłowski  and K Rzążewski 

Center for Theoretical Physics, Polish Academy of Sciences, Al. Lotników 32/46, 02-668 Warsaw, Poland

¹ Author to whom any correspondence should be addressed.E-mail: rafal@cft.edu.pl

Keywords: dipolar interactions, 1D systems, roton, ultracold gases

Abstract

We solve numerically exactly the many-body 1D model of bosons interacting via short-range and dipolar forces and moving in the box with periodic boundary conditions. We show that the lowest energy states with fixed total momentum can be smoothly transformed from the typical states of collective character to states resembling single particle excitations. In particular, we identify the celebrated roton state. The smooth transition is realized by simultaneous tuning short-range interactions and adjusting a trap geometry. With our methods we study the weakly interacting regime as well as the regime beyond the range of validity of the Bogoliubov approximation.

1. Introduction

In the 30s of the last century unusual properties of the Helium-II were discovered. The subsequent results of Allen and Misener [1], Kapitza [2] were simulating the development of theoretical models [3–7]. The qualitative theory of superfluidity is due to Landau [5–7]. He deduced from the measurement of the specific heat [8] and the second sound velocity [9] that the excitations in the Helium-II must have a peculiar spectrum, with the local minimum [7]. The excitation at the local minimum has been called a ‘roton’. Later Feynman alone [10] and with Cohen [11] formulated the very first, yet semiquantitative microscopic model explaining the origin of this local minimum. Finally, in Helium the roton was observed experimentally [12], but rather unsatisfactory agreement between theory and measurement suggested that the exact nature of the rotonic excitation was still missing. It was finally understood many years later by means of subtle ansatzes for the roton’s wave function [13, 14]. The existence and properties of the roton were also discussed in depth in studies of excitations of thin liquid-helium films [15–17]. It should be emphasized that liquid Helium-II is a strongly correlated (with a small condensate fraction) system, where roton’s characteristic momentum scales as the interatomic distance. There are still active studies of the roton state in this regime [18].

At the beginning of XXI century the roton-maxon spectrum was predicted in completely different physical system—dipolar gas of polarized ultracold atoms. The nature of the roton in ultracold gases is very different than the one in Helium (see [19] for detailed discussion). Here it is induced by the interplay between the long-range forces and a steep external potential in the polarization direction [20, 21]. Without an external potential the system is unstable, as the dipoles would first tend to the head to tail configuration and then they will just fall on each other due to the attractive part of the dipolar interaction. The system may be stabilized by the steep external potential, which blocks the motion in the direction of the dipoles’ polarization. Roton emerges for parameters close to collapse, for which dipoles are close to overcome the trapping forces. In this situation atoms cluster into ‘clumps’, regularly separated by a period corresponding to inverse of the roton momentum [22]. This happens for relatively weak interactions, for which the system is in the Bose–Einstein condensate state. Therefore, one can use the mean field or Bogoliubov description and find the roton state as a Bogoliubov quasi particle [20–39]. The dispersion curve of such systems is related to a specific k -dependence of an effective interaction potential rather than to strong correlations. Possibility of changing the particles polarization as well as almost free tuning of the short-range interactions combined with the trap geometry modifications enables unprecedented flexibility in the study of the roton spectrum in dipolar gases [20–39] ending with a recent experimental confirmation of the phenomenon [40]. Usually the dipolar system is studied within the Bogoliubov approximation, so that there is

no access to the detailed structure of the low-lying excitations. Only a few many-body investigations were performed for the roton state using different techniques [41–44]. A good attempt can be made by a numerically exact solution to a many-body problem with a rotonic characteristic. Even if found for relatively small number of particles, modern experiments with a precise control over only a few atoms in optical lattices or single traps (see for instance [45–49]) allow to test its physical predictions.

In this work we present numerically exact results for a quasi-1D model, which admits the roton excitation. In a number of recent papers low excitation of 1D interacting bosons were already investigated (see for instance [50–55] and references therein). The historically earliest example is the famous Lieb–Liniger model [56, 57] comprising of N contact interacting bosons moving on the circle. Their seminal analytical solution predicts two branches of elementary excitations, which was also observed experimentally [47]. The upper type-I excitation branch was immediately recognized as the Bogoliubov excitation spectrum [58]. The states of the lower type-II excitation branch, were identified later with gray and dark solitons arising in the mean field theory of ultracold gases [59–62]. Little is known about the classification of the exact many-body elementary excitations in the dipolar gas. For (quasi)-1D model with bosons interacting only by repulsive dipolar interactions the lowest energy states resemble rather type-II excitations known from the Lieb–Liniger model [53, 63] and for at least weakly interacting regime the picture with two branches of elementary excitations is also expected in this case [64]. On the other hand, in the dipolar systems, well understood Bogoliubov spectrum may exhibit a local minimum identified as a roton [20, 21]. When the interatomic forces are of the attractive character on the short-scale, whereas the long-range part of potential is repulsive, the interplay of these two interactions may lower the energy of the roton mode even to the ground state level. It opens a significant question: is it possible in a dipolar analog of the Lieb–Liniger model that the two branches cross, such that it is a type-I Bogoliubov excitation, in particular the roton, which would appear in the lower branch?

It is a purpose of this work to show that by tuning short-range interactions and adjusting a ring geometry one can continuously change [65] the character of the lowest energy state for a given total momentum of the system from a type-II excitation to the roton mode. We also analyze a numerically exact roton’s wave function in the weakly interacting regime and its position and momentum properties.

2. Model

We consider N dipolar bosons confined in both transverse directions \hat{y} and \hat{z} with a tight harmonic trap of a frequency ω_{\perp} . Multi particle wave function is approximately the Gaussian in tight directions for all variables. It requires the chemical potential μ much smaller than energy of the first excited state in the transverse direction, $\mu \ll \hbar\omega_{\perp}$. In the longitudinal direction \hat{x} the space is assumed to be finite, with the length L and with the periodic boundary conditions imposing quantization of momenta in that direction. All atoms are polarized along the \hat{z} axis. The above system corresponds to atoms moving on the circumference of a circle, having the dipole moments perpendicular to the circle-plane. Hence, in analogy with nuclear physics [66, 67] and following [59, 60] we call the lowest energy states of a given total momentum of the system, the yrast states. Our quasi-1D system is governed by Hamiltonian

$$\hat{H} = \sum_k \frac{\hbar^2 k^2}{2m} \hat{a}_k^{\dagger} \hat{a}_k + \frac{1}{2L} \sum_{k_1, k_2, k} \hat{a}_{k_1+k}^{\dagger} \hat{a}_{k_2-k}^{\dagger} V_{\text{eff}}(k) \hat{a}_{k_1} \hat{a}_{k_2}, \quad (1)$$

with \hat{a}_k (\hat{a}_k^{\dagger}) annihilating (creating) a boson with momentum k . The effective potential consists of the long-range dipolar part and the short-range part, namely $V_{\text{eff}}(k) = V_{\text{sr}}(k) + V_{\text{dd}}(k)$.

The quasi-1D dipolar potential reads $V_{\text{dd}}(k) = \frac{3\hbar^2 a_{\text{dd}}}{m l_{\perp}^2} (1 + f((l_{\perp} k)^2/2))$ with $l_{\perp} = \sqrt{\hbar/m\omega_{\perp}}$. The parameter $a_{\text{dd}} = m\mu_0 d^2/(12\pi\hbar^2)$ is a ‘dipole length’, where d is an atomic dipole moment and μ_0 is the vacuum permeability. This effective quasi-1D potential comes from integration of the full 3D dipolar interaction over both transverse variables. The singular part coming from this integration is incorporated with the short-range interaction. The function f which appears in equation (1) is equal to $f(u) = u e^u \text{Ei}(u)$, where Ei is the exponential integral [68].

Stability of our calculations requires smoothing of a usual short-range interaction model used in the ultracold physics, the delta function. We choose a Gaussian model [69–77], namely $V_{\text{sr}}(k) = V_0 e^{-\frac{1}{2}k^2 r^2}$ with r standing for the potential range and $|V_0|$ for its depth ($V_0 \leq 0$ later in this work). This step makes our model more realistic, imitating the attractive van der Waals interaction. Note, that our short-range potential interaction produces zero force at $x = 0$, thus the growing kinetic energy of the narrowing wave packet prevents the system from the collapse. This indicates that our Hamiltonian is bounded from below. For convenience we set $V_0 = \frac{\hbar^2 a}{m l_{\perp}^2}$ with $a \leq 0$ mimicking an usual scattering length, which can be tuned in experiments by Feshbach resonances. The relation between Gaussian model parameters a , r and the real scattering length can be found in

[78] and references therein. Below we use box units where $L/2\pi$, $2\pi\hbar/L$ and $4\pi^2\hbar^2/mL^2$ are the units of length, momentum and energy, respectively.

Our effective potential $V_{\text{eff}}(k)$ corresponds to calculating the interactions along the circumference positions with the periodicity of the system accounted for. However, we checked that it would not be changed significantly if a bit elegant but more realistic geometric distance over the chord was used (see appendix A).

We access the many-body eigenstates of Hamiltonian (1) by exact diagonalization using the Lanczos algorithm [79]. Our calculations are performed in the Fock space spanned by the plane-wave basis with a maximum total kinetic energy of the system $E_{\text{max}} = k_{\text{max}}^2/2$ —with single-particle momentum $k_{\text{max}} \gg 1/r$ —sufficiently high to assure convergence. Here we employ the fact that the total momentum of the system $\hat{K} = \sum_k k \hat{a}_k^\dagger \hat{a}_k$ is conserved, $[\hat{H}, \hat{K}] = 0$, so its eigenvalues K are good quantum numbers, used here together with the total number of atoms N to label different eigenstates $|N, K, i\rangle$ enumerated by i with $i = 0$ corresponding to a yrast state. We remind the Reader that for finite systems on the ring it suffices to consider the eigenstates only up to $K/N = 1/2$ [57, 60]. This comes from the presence of the so called *umklapp* process [57]. Any eigenstate with a total momentum $K' = p \cdot N + K$ (where $p \in \mathbb{Z}$, $-\frac{N}{2} \leq K \leq \frac{N}{2}$) may be understood as the state with a total momentum K with a shifted center-of-mass momentum (see figure 5 in [60]). Note that such shifting does not change the internal structure of the state.

3. Results

In the following paragraphs of this work we consider two different situations, namely with weak interactions where the depletion (given by $P(K = 0)$ in figures 1(d) and 2(d)) of a ground state is less than 5% and stronger interactions where its value is around 20%. Note, that the latter case is still far from the Helium-II regime. We present in figure 1 our analysis of yrast states for the first situation. We consider $N = 16$ dysprosium atoms with $a_{\text{dd}} = 132 a_0$ and the potential range $r = 182 a_0$, where a_0 is the Bohr radius. The value of r , in this case, equals the characteristic length of the attractive part of van der Waals interactions for dysprosium atoms [80]. We initially set a and ω_\perp corresponding to the usual situation where the yrast states rather resemble the lowest excitation branch from the Lieb–Liniger model [63, 64] and compare their energies (black squares in figure 1(a)) with the Bogoliubov spectrum (black dashed line) given by:

$$\epsilon_k = \sqrt{\frac{k^2}{2} \left(\frac{k^2}{2} + 2NV_{\text{eff}}(k) \right)}. \quad (2)$$

Then we continuously change a and ω_\perp (a similar effect would be observed if one changed the length of the box) keeping $V_{\text{eff}}(0) = \text{const.}$ We finally end with the profoundly different spectrum (red points in figure 1(a)) with the characteristic inflection point for $K = 2$. Our result suggest that at least some of yrast states may change their character from collective type-II excitations [63] to type-I ones. Moreover, we argue that the inflection point can be identified with the roton-like state.

To test our hypothesis about the change of the character of the yrast state for $K = 2$ we compare it together with the first excited state with the particle number conserving Bogoliubov approximation [81] sketched here briefly. The spectrum in the Bogoliubov approximation is explained by the concept of quasiparticles that, in our case, has to be rewritten in terms of Fock states in particle basis. We use the following Ansatz [82] for the Bogoliubov vacuum ($K = 0$):

$$|0\rangle_B \propto \left(\hat{a}_0^\dagger \right)^2 - 2 \sum_{k>0} \frac{v_k}{u_k} \hat{a}_k^\dagger \hat{a}_{-k}^\dagger \Big)^{N/2} |\text{vac}\rangle, \quad (3)$$

where $|\text{vac}\rangle$ is the particle vacuum and $u_k, v_k = (\sqrt{\epsilon_k/E_k} \pm \sqrt{E_k/\epsilon_k})/2$ with $E_k = k^2/2$. A single Bogoliubov excitation with a total momentum K is expressed by $|N, K\rangle_B \propto (u_K \hat{a}_0 \hat{a}_K^\dagger + v_K \hat{a}_0^\dagger \hat{a}_{-K}) |0\rangle_B$. To trace a continuous transformation of the yrast state from type-II to type-I excitation we evaluate the fidelities $|\langle N, K, i | N, K \rangle_B|^2$, which is depicted in figure 1(b). For the initial values of the parameters a and ω_\perp the first excited state is a Bogoliubov excitation, whereas the yrast state remains a type-II excitation [63]—a fact observed in the Lieb–Liniger result as well. Then we observe a gradual exchange of the states' character as we modify the effective potential ending with a complete role reversal of the two first states. Note, that the sum of the fidelities (black dotted line in figure 1(b)) is almost equal to 1 at any stage of the transition. It means that Bogoliubov excitation, to a good approximation, remains in a plane spanned by the two lowest eigenstates.

To show the qualitative change of the yrast state for $K = 2$ we calculate the normalized normally ordered second order correlation function (widely used in the quantum optics) $g_2(x) := \langle \Psi^\dagger(x) \Psi^\dagger(0) \Psi(0) \Psi(x) \rangle / \langle \Psi^\dagger(x) \Psi(x) \rangle \langle \Psi^\dagger(0) \Psi(0) \rangle$ (figure 1(c)), which can be measured in experiments with ultracold atoms, see for instance [83–86].

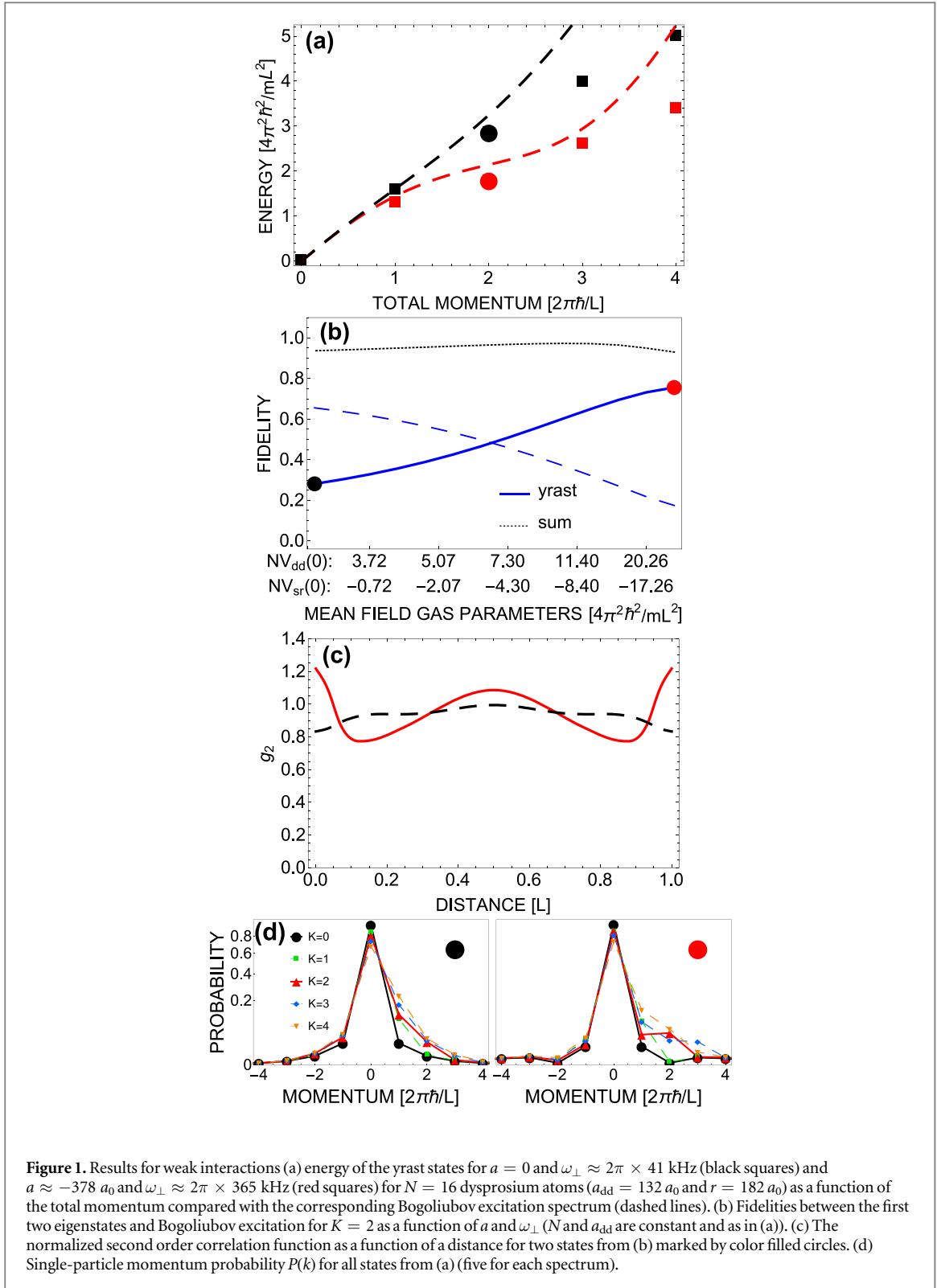


Figure 1. Results for weak interactions (a) energy of the yrast states for $a = 0$ and $\omega_{\perp} \approx 2\pi \times 41$ kHz (black squares) and $a \approx -378 a_0$ and $\omega_{\perp} \approx 2\pi \times 365$ kHz (red squares) for $N = 16$ dysprosium atoms ($a_{dd} = 132 a_0$ and $r = 182 a_0$) as a function of the total momentum compared with the corresponding Bogoliubov excitation spectrum (dashed lines). (b) Fidelities between the first two eigenstates and Bogoliubov excitation for $K = 2$ as a function of a and ω_{\perp} (N and a_{dd} are constant and as in (a)). (c) The normalized second order correlation function as a function of a distance for two states from (b) marked by color filled circles. (d) Single-particle momentum probability $P(k)$ for all states from (a) (five for each spectrum).

We observe a dramatic difference between two yrast states for border cases from figure 1(b) (marked as black and red points). Namely that almost flat distribution typical for type-II excitation in weakly interacting regime is replaced by a function exhibiting an enhanced regular modulation with the number of maxima given by K_{rot} , which is the roton momentum. We have the following interpretation of this behavior. The function $g_2(x)$ is related to the probability of finding a particle at position x provided that the first one was measured at $x = 0$. We expect that the second order correlation function should have modulation with periodicity depending on the typical non-zero single particle momenta in the system. The value of a single particle momenta is a random variable given by distribution, which is often not peaked at the total momentum of the system (as discussed in details below). Therefore the modulation in g_2 function, if there is any, does not have to correspond to the total

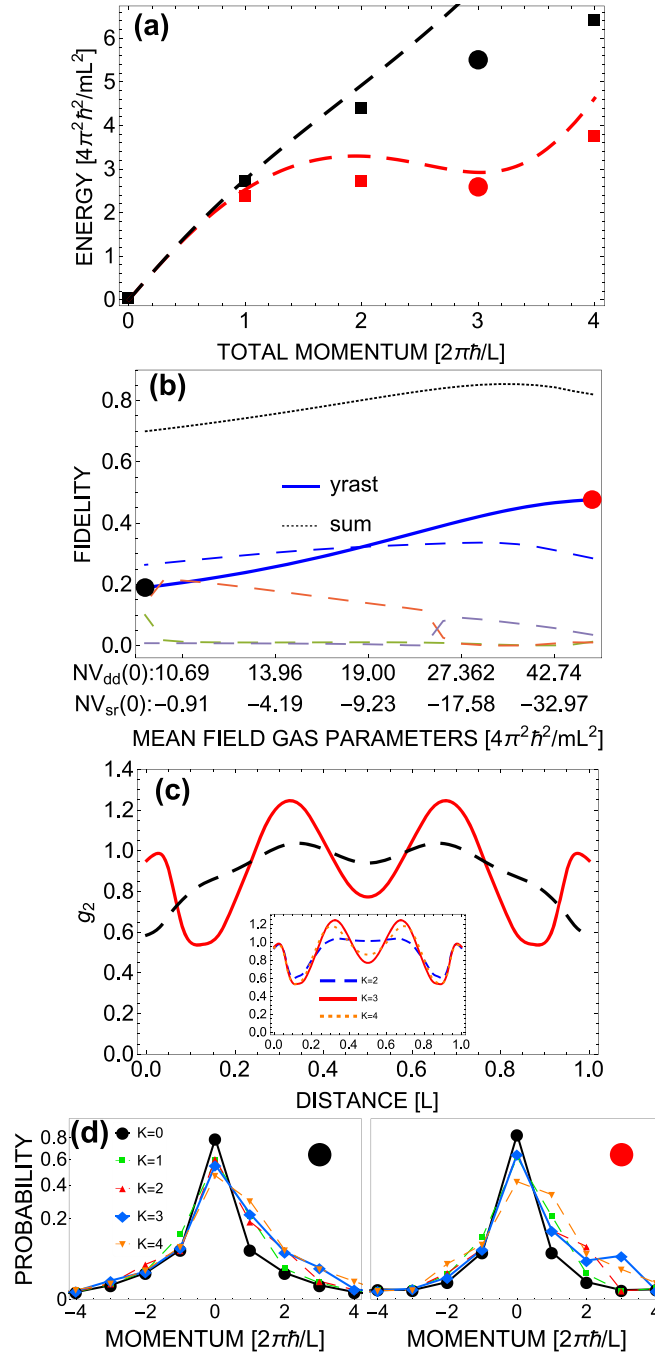
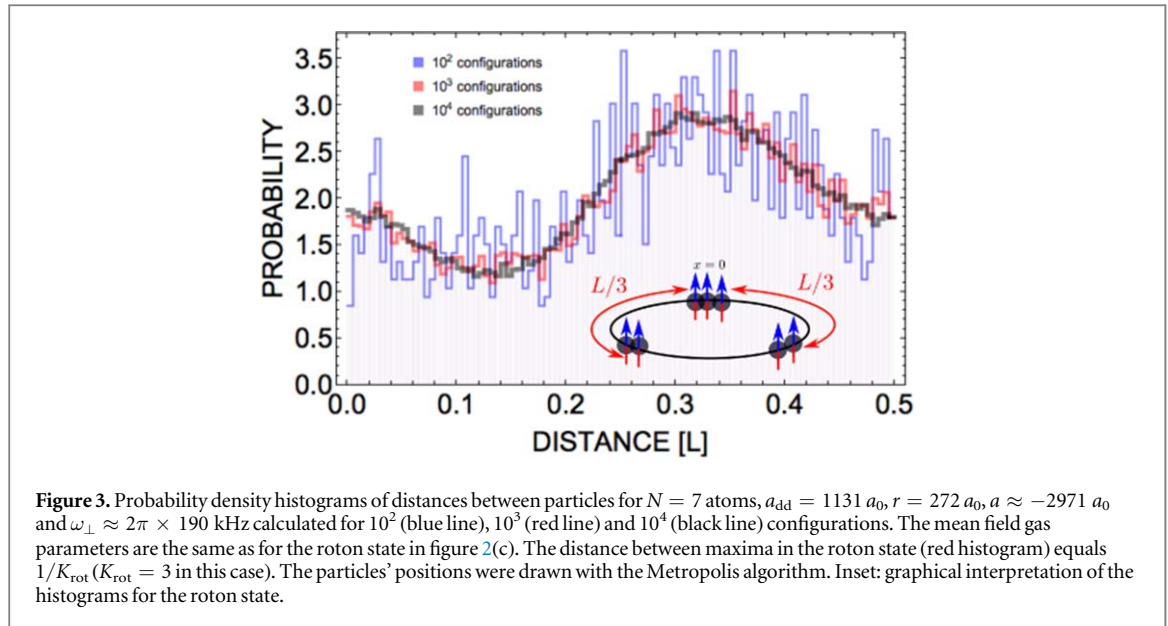


Figure 2. Results for stronger interactions (a) energy of the yrast states for $a = 0$ and $\omega_{\perp} \approx 2\pi \times 35$ kHz (black squares) and $a \approx -2080 a_0$ and $\omega_{\perp} \approx 2\pi \times 190$ kHz (red squares) for $N = 10$ atoms ($a_{dd} = 792 a_0$ and $r = 272 a_0$) as a function of the total momentum compared with the corresponding Bogoliubov excitation spectrum (dashed lines). (b) Fidelities between the first five eigenstates and Bogoliubov excitation for $K = 3$ as a function of a and ω_{\perp} (N and a_{dd} are constant and as in (a)). (c) The normalized second order correlation function as a function of a distance for two states from (b) marked by color filled circles. Inset: comparison between yrast states $K = 2$ (dashed blue line), $K = 3$ (orange dotted line) and $K = 4$ (red line) for the spectrum with the local minimum (d) single-particle momentum probability $P(k)$ for all states from (a) (five for each spectrum).

momentum K . In this respect the Bogoliubov excitations, i.e. states $\hat{b}_{k=K}^{\dagger}|\text{vac}\rangle$, are special, because a typical non-zero single-particle momentum is equal to the total momentum of the system. The fact that the g_2 function of the yrast state with $K = 2$ has also modulation with period $1/K$ ensure us that we deal with a Bogoliubov excitation in the yrast states' branch.

Note, that for a small number of particles we are able to find stable solutions corresponding to realistic mean field gas parameters ($NV_{sr}(0) = -23.98$, $NV_{dd}(0) = 26.98$) only for the Bogoliubov spectrum with the inflection, not to the one with the characteristic local minimum. Using the mean field gas parameters ($NV_{sr}(0)$,



$NV_{dd}(0)$ for which the Bogoliubov spectrum has the local minimum implies much stronger interactions for our few-body system. Our result would approach Bogoliubov's predictions in the limit of $N \rightarrow \infty$ (see appendix B).

Here, we turn to the strong interactions scenario with $N = 10$, which is beyond the Bogoliubov approximation. In figure 2 we summarize our findings, where the characteristic local minimum for $K = 3$ is present. In this case the spectrum is calculated with an accuracy of several percent only. Our previous conclusions hold also for this situation. However, the role reversal of the lowest states is more subtle because of higher momentum of the roton. At the end of the transition we stay with the yrast state, which still has the overlap with Bogoliubov (50%). As in the previous case, the second order correlation function of our candidate for roton exhibits the enhanced regular modulation with periodicity corresponding to $1/K_{\text{rot}}$, where $K_{\text{rot}} = 3$ is the position of the minimum in the spectrum (figure 2(a)) and the total momentum of the yrast state. In the inset of figure 2(c) we show the second order correlations functions of the yrast states with $K = 2$ or $K = 4$, which also have traces of the modulations with a period $1/K_{\text{rot}}$.

The spectrum and modulation of the second order correlation function indicate that we still have a roton-like state, even though this regime is beyond the Bogoliubov approximation validity range.

How does the calculated g_2 function correspond to an experimental imaging of particles positions using a CCD camera? Having a many-body wave function of a given eigenstate, in particular the roton state, we can explore a multivariate probability distribution of particles positions in a following way [62, 64]. Using Metropolis algorithm we draw N positions from the multi particle probability distribution $|\Psi_{NK}^i(\vec{x})|^2 = |\langle \vec{x} | N, K, i \rangle|^2$ where $\vec{x} = (x_1, \dots, x_N)$ is a position vector of N particles and $\Psi_{NK}^i(\vec{x})$ is the many-body eigenstate in a position representation. We repeat this procedure many times, collecting configurations $\{\vec{x}\}_i = \{\vec{x}_1^i, \dots, \vec{x}_N^i\}$ from each (i th) shot. In the experiment it corresponds to measuring N th order correlation function. Due to the ring geometry it would be hard to average it as the center of mass for each $\{\vec{x}\}_i$ is randomly placed in accordance with a rotationally uniform distribution [64]. On the other hand, the distances between particles in each configuration are translationally invariant and may reveal any potentially hidden pair correlations for a given eigenstate. Indeed, the probability distribution of the inter particle distances is directly related to the $g_2(x)$ function. How many samples one needs to estimate it? In figure 3 we compare probability distribution function histograms of distances between particles in each configuration $\{\vec{x}\}_i$ 'measured' numerically for different number of configurations involved in average calculated for the roton state with the mean field gas parameters identical to the ones from figure 2(c) ($K_{\text{rot}} = 3$), but obtained for $N = 7$ particles due to the factorial growth of terms in the expression for the many-body wave function with N . The distance between i th and j th particle is defined as: $d_{ij} = \min(|x_i - x_j|, 1 - |x_i - x_j|)$ with $0 \leq d_{ij} \leq 0.5$. As we can see the results converge rather fast as we increase number of configurations involved. The inset of figure 3 explains why we observe only the local maximum for $x = 1/3L$ in the histograms and not for $x = 2/3L$ also. It is simply because of our natural definition of distance between particles on a ring geometry.

Note that the presence, position, and depth of the roton minimum for both cases considered in this work are tunable by varying the number of atoms N , trapping frequency ω_{\perp} and the short-range coupling strength as it was predicted for the roton state in the mean field studies of ultracold dipolar gases [20]. We choose

$K_{\text{rot}}/N < 1/2$ to minimize the impact of the *umklapp* process [57], discussed earlier in this work, on the eigenstates.

To fully comprehend the difference between the two types of low-energy excitations we study the probability $P(k) = \frac{1}{N} \langle \hat{a}_k^\dagger \hat{a}_k \rangle$ of finding a single-particle moving with momentum k for yrast states with various K . For both weak and strong interactions the type-II yrast states (black markers in figures 1(d) and 2(d)) for $K > 1$ beside $k = 0$ mainly consists of $k = 1$ states, which is more visible as we increase K . It corresponds to a dominant role of one of the Dicke states (exactly K atoms with $k = 1$ and $N - K$ with $k = 0$) in their many-body wave function [63, 64], especially for weak interactions. On the other hand, in the rotonic cases (red markers in figures 1(d) and 2(d)) we observe a local maximum of $P(k)$ for $k = K_{\text{rot}}$ for the yrast states with K_{rot} , which clearly resembles recently published result by Ferlaino's group [40]. It means that the yrast state for K_{rot} has a single particle excitation character rather than a collective one, so that within our, experimentally achievable, procedure one can completely change the character of the low-energy excitations.

4. Discussion

We find with our numerically exact treatment that all the properties of the roton state discussed earlier can be understood by analyzing contributions of different Fock states to its wave function. In both cases of interactions studied in this work, we find that the dominant contribution to the roton states comes from the so called W state $|0_{-k_{\text{max}}}, \dots, (N-1)_0, 0_1, 1_2, \dots, 0_{k_{\text{max}}}\rangle$, as one would expect for the Bogoliubov excitations [64]. The latter state is important from the fundamental point of view, as representative of an entanglement class [87], and applied side—it can be used to beat the standard quantum limit for the metrological tasks [88]. The state was recently produced via non-demolition measurement [89]. According to our earlier findings [64], which holds also for purely dipolar repulsion [63], the low-lying excitations of weakly interacting bosons are highly-entangled states dominated by the Dicke state, a result of the bosonic statistics mainly. However, the interplay between the short-range and long-range interactions of the opposite sign can promote the excitation with the dominant W state as a low-lying excitation for $K > 1$ in the system.

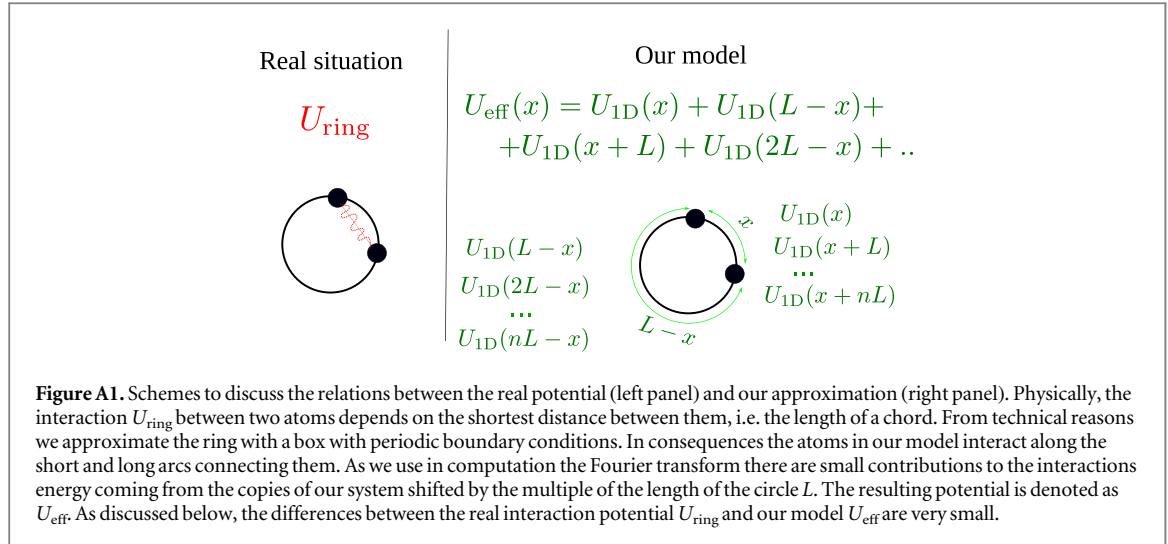
As we can see in the appendix B the features of the many-body problem solution depends on the value of the mean field gas parameters rather than the number of atoms itself as long as the depletion of the system is not big (it is getting smaller and smaller as we increase a number of atoms). This makes our results for relatively small number of particles, stronger interactions and tight trapping frequencies easier to verify experimentally. For example if one wants to confirm our predictions for spectrum for the roton with the mean field parameters as in figure 2(a), $K_{\text{rot}} = 3$, $N = 600$ and a ring of $5 \mu\text{m}$ length, it will require usage of dysprosium atoms with $a_{\text{dd}} = 132 a_0$ and $\omega_{\perp} \approx 2\pi \times 1.9 \text{ kHz}$ and tuning the short-range scattering length with Feshbach resonances.

5. Conclusion

To summarize, we showed that manipulating physical parameters in our model one can continuously alter the character of a given yrast state from type-II excitation to the roton mode. We emphasize the fact that the effect is already present in relatively small systems enabling use of the simplest exact diagonalization of the whole Hamiltonian. All interesting properties of the roton-like mode both in the momentum and the position representations come from the fact, that the W state plays the dominant role in the roton state in the plane wave basis. It is in the stark contrast to the weakly repulsive bosons, where the dominant role of the Dicke states is observed [63, 64]. We show that the normalized second order correlation function, accessible in experiments, displays characteristic enhanced regular modulation for the roton state. Within our many-body model we access stronger regimes between the weakly interacting one and the Helium-II scenario, finding the roton mode also in this case. Our results open new questions concerning quasi-1D systems with both long-range and short-range interactions. Is it possible to fully replace type-II branch with type-I branch as low-lying excitations? Would solitonic branch still exist in the spectrum? The thermodynamic properties of dipolar bosons were investigated only approximately, in the weakly interacting regime [90–92]. The results presented in this paper can motivate further research in this direction, but using full many-body approach accounting for the lower branch and the transitions discussed here.

Acknowledgments

We acknowledge fruitful discussions with K Sacha, A Syrwid, A Sinatra and Y Castin. This work was supported by the (Polish) National Science Center Grants 2016/21/N/ST2/03432 (RO and WG), 2014/13/D/ST2/01883 (KP) and 2015/19/B/ST2/02820 (KR).



Appendix A. The effective potential. Realistic versus periodic

In reality particles trapped in the ring-shaped potential would interact via interaction potential depending on the shortest distance between them, the length of a chord. As we replace the ring with a box with periodic boundary condition, the effective potential used in the main text (in the momentum representation) $V_{\text{eff}}(k)$ is only approximate model of the physical interaction. We explain the qualitative differences, between the physical interaction potential and our model in figure A1. Below we give details how our model $V_{\text{eff}}(k)$ arises, and compare it with the real potential. We use the symbol U for the potentials in the position representation and V for potentials in the momentum space.

Let us start from purely theoretical situation, where atoms are confined in both transverse directions \hat{y} and \hat{z} with a tight harmonic trap but in the longitudinal direction \hat{x} the space is infinite. Then one-dimensional potential $U_{1\text{D}}(x)$ takes the form:

$$U_{1\text{D}}(x) = \frac{\hbar^2 a}{m_{\perp}^2} \frac{g(x/r)}{r} + \frac{\hbar^2 a_{\text{dd}}}{m_{\perp}^2} \frac{h(x/L_{\perp})}{L_{\perp}} \quad \text{where}$$

$$g(q) = \frac{1}{\sqrt{2\pi}} e^{-\frac{q^2}{2}},$$

$$h(q) = \frac{3}{4} \left(-2|q| + \sqrt{2\pi} (1 + q^2) e^{\frac{q^2}{2}} \text{Erfc} \left(\frac{|q|}{\sqrt{2}} \right) \right). \quad (\text{A.1})$$

In real experiment, when space need to be finite, atoms are trapped in the ring shaped potential (as we want to avoid breaking translational invariance). Therefore they interact via potential depending on the length of the chord (see left panel in figure A1):

$$U_{\text{ring}}(x) = U_{1\text{D}} \left(\frac{L}{\pi} \sin \left(\frac{\pi x}{L} \right) \right). \quad (\text{A.2})$$

In this work, from technical reasons, we model such situation by a box of length L with periodic boundary conditions. We introduce effective potential, which includes interaction with all imaginary copies of system:

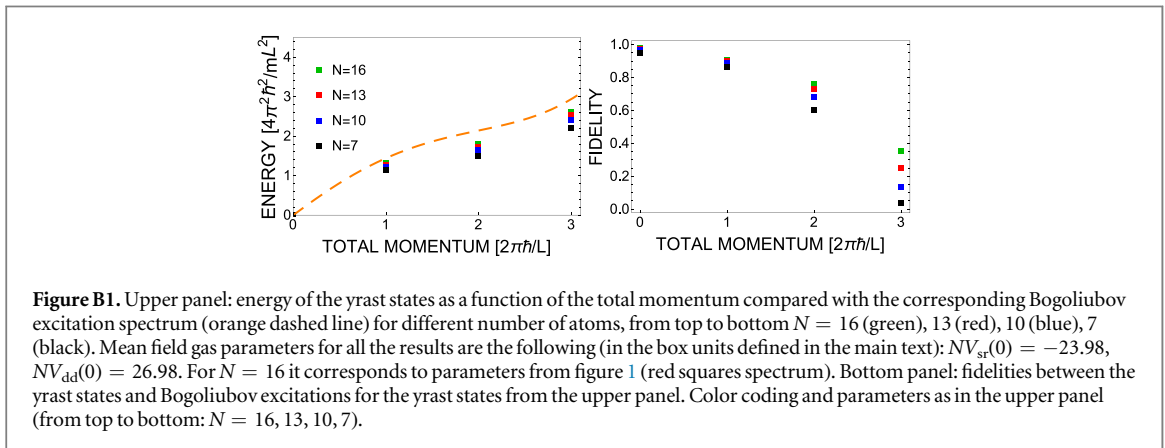
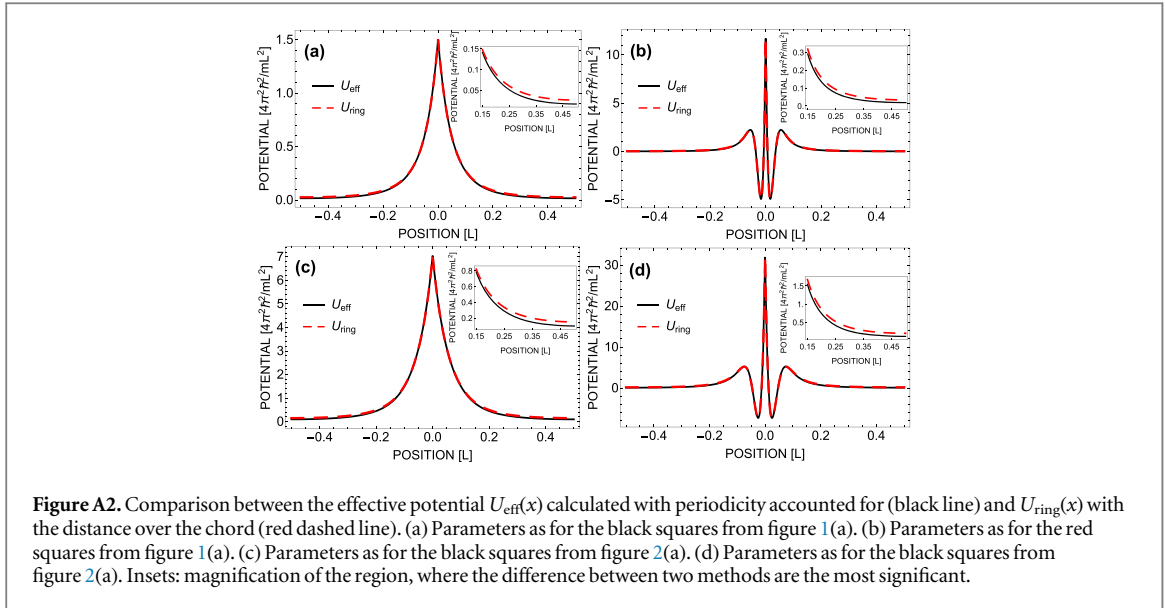
$$U_{\text{eff}}(x) = \sum_{n \in \mathbb{Z}} U_{1\text{D}}(x + nL). \quad (\text{A.3})$$

Therefore, the effective potential in momentum representation is $V_{\text{eff}}(k) = \int_0^L e^{-ikx} U_{\text{eff}}(x) dx$ (which satisfies $V_{\text{eff}}(k) = \mathcal{F}(U_{1\text{D}})(k)$ as well).

In figure A2 we compare both approaches. As we see both curves are almost indistinguishable in the regions where the value of the effective potential is meaningful. A very small difference in all cases from figure A2 is observed only on the potential tail.

Appendix B. Convergence towards $N \rightarrow \infty$ limit

In the Bogoliubov approximation one operates with the mean field gas parameters $NV_{\text{sr}}(0)$, $NV_{\text{dd}}(0)$ (in the box units defined in the main text) with the assumption of weak interactions and large number of atoms N .



Obviously, in the many-body approach, where N is finite, the energy of the pairwise interactions is significantly higher. Then, one can ask how many atoms (how weak interactions) one needs to converge with the many-body solution towards $N \rightarrow \infty$ limit. To answer it, we study energies of a series of yrast states (left panel of figure B1) and their overlaps with the corresponding Bogoliubov excitations given by fidelities (right panel of figure B1) defined in the main text. We obtain both the spectrum and the fidelities for different number of atoms N ranging from 7 to 16. The parameters for different N are chosen to always produce the same Bogoliubov excitation spectrum with the inflection point as for red dashed line in figure 1(a) in the main text. We see that even for small number of atoms $N = 16$ we obtain very good overlap with the Bogoliubov approximation, especially for $K \leq 2$. However, our numerically exact solution includes all the possible correlations between atoms, hence it cannot be fully reproduced by single Bogoliubov excitation.

ORCID iDs

R Ołdziejewski  <https://orcid.org/0000-0001-5094-2854>

K Pawłowski  <https://orcid.org/0000-0001-6412-4457>

K Rzażewski  <https://orcid.org/0000-0002-6082-3565>

References

- [1] Allen J and Misener A 1938 *Nature* **141** 75
- [2] Kapitza P 1938 *Nature* **141** 74
- [3] London F 1938 *London* **141** 643
- [4] Tisza L 1938 *Nature* **141** 913
- [5] Landau L 1941 *Phys. Rev.* **60** 356

- [6] Landau L 1941 *J. Phys.* **5** 71
- [7] Landau L 1947 *J. Phys.* **11** 91
- [8] Kapitza P L 1941 *Phys. Rev.* **60** 354
- [9] Peshkov V 1946 *J. Phys.* **10** 389
- [10] Feynman R P 1954 *Phys. Rev.* **94** 262
- [11] Feynman R P and Cohen M 1956 *Phys. Rev.* **102** 1189
- [12] Henshaw D and Woods A 1961 *Phys. Rev.* **121** 1266
- [13] Galli D E, Cecchetti E and Reatto L 1996 *Phys. Rev. Lett.* **77** 5401
- [14] Apaja V and Saarela M 1998 *Phys. Rev. B* **57** 5358
- [15] Epstein J L and Krotscheck E 1988 *Phys. Rev. B* **37** 1666
- [16] Clements B E, Godfrin H, Krotscheck E, Lauter H J, Leiderer P, Passioux V and Tymczak C J 1996 *Phys. Rev. B* **53** 12242
- [17] Clements B E, Krotscheck E and Tymczak C J 1996 *Phys. Rev. B* **53** 12253
- [18] Rota R, Tramonto F, Galli D E and Giorgini S 2013 *Phys. Rev. B* **88** 214505
- [19] Wilson R M 2011 Manifestations of the roton in dipolar Bose–Einstein condensates *PhD Thesis* University of Colorado at Boulder
- [20] Santos L, Shlyapnikov G V and Lewenstein M 2003 *Phys. Rev. Lett.* **90** 250403
- [21] O’Dell D H J, Giovanazzi S and Kurizki G 2003 *Phys. Rev. Lett.* **90** 110402
- [22] Bohn J L, Wilson R M and Ronen S 2009 *Laser Phys.* **19** 547
- [23] Fischer U R 2006 *Phys. Rev. A* **73** 031602
- [24] Ronen S, Bortolotti D C and Bohn J L 2007 *Phys. Rev. Lett.* **98** 030406
- [25] Wilson R M, Ronen S, Bohn J L and Pu H 2008 *Phys. Rev. Lett.* **100** 245302
- [26] Bohn J L, Wilson R M and Ronen S 2009 *Laser Phys.* **19** 547
- [27] Parker N, Ticknor C, Martin A and O’Dell D 2009 *Phys. Rev. A* **79** 013617
- [28] Wilson R M, Ronen S and Bohn J L 2010 *Phys. Rev. Lett.* **104** 094501
- [29] Nath R and Santos L 2010 *Phys. Rev. A* **81** 033626
- [30] Klawunn M, Recati A, Pitaevskii L and Stringari S 2011 *Phys. Rev. A* **84** 033612
- [31] Martin A and Blakie P 2012 *Phys. Rev. A* **86** 053623
- [32] Blakie P, Baillie D and Bisset R 2012 *Phys. Rev. A* **86** 021604
- [33] Jona-Lasinio M, Łakomy K and Santos L 2013 *Phys. Rev. A* **88** 013619
- [34] Bisset R, Baillie D and Blakie P 2013 *Phys. Rev. A* **88** 043606
- [35] Bisset R and Blakie P 2013 *Phys. Rev. Lett.* **110** 265302
- [36] Jona-Lasinio M, Łakomy K and Santos L 2013 *Phys. Rev. A* **88** 025603
- [37] Corson J P, Wilson R M and Bohn J L 2013 *Phys. Rev. A* **87** 051605
- [38] Blakie P, Baillie D and Bisset R 2013 *Phys. Rev. A* **88** 013638
- [39] Natu S S, Campanello L and Sarma S D 2014 *Phys. Rev. A* **90** 043617
- [40] Chomaz L, Bijnen R, Petter D, Faraoni G, Baier S, Becher J, Mark M, Wächtler F, Santos L and Ferlaino F 2018 *Nat. Phys.* **14** 442
- [41] Astrakharchik G E, Boronat J, Kurbakov I L and Lozovik Y E 2007 *Phys. Rev. Lett.* **98** 060405
- [42] Mazzanti F, Zillich R E, Astrakharchik G E and Boronat J 2009 *Phys. Rev. Lett.* **102** 110405
- [43] Hufnagl D, Krotscheck E and Zillich R E 2009 *J. Low Temp. Phys.* **158** 85
- [44] Cinti F, Jain P, Boninsegni M, Micheli A, Zoller P and Pupillo G 2010 *Phys. Rev. Lett.* **105** 135301
- [45] Greiner M, Mandel O, Esslinger T, Hänsch T W and Bloch I 2002 *Nature* **415** 39
- [46] Serwane F, Zürn G, Lompe T, Ottenstein T, Wenz A and Jochim S 2011 *Science* **332** 336
- [47] Meinert F, Panfil M, Mark M J, Lauber K, Caux J-S and Nägerl H-C 2015 *Phys. Rev. Lett.* **115** 085301
- [48] Baier S, Mark M J, Petter D, Aikawa K, Chomaz L, Cai Z, Baranov M, Zoller P and Ferlaino F 2016 *Science* **352** 201
- [49] Baier S, Petter D, Becher J, Patscheider A, Natale G, Chomaz L, Mark M and Ferlaino F 2018 *Phys. Rev. Lett.* **121** 093602
- [50] Astrakharchik G E, Boronat J, Casulleras J and Giorgini S 2005 *Phys. Rev. Lett.* **95** 190407
- [51] Caux J-S and Calabrese P 2006 *Phys. Rev. A* **74** 031605
- [52] Astrakharchik G E and Lozovik Y E 2008 *Phys. Rev. A* **77** 013404
- [53] De Palo S, Orignac E, Citro R and Chiofalo M 2008 *Phys. Rev. B* **77** 212101
- [54] Imambekov A, Schmidt T L and Glazman L I 2012 *Rev. Mod. Phys.* **84** 1253
- [55] Girardeau M D and Astrakharchik G E 2012 *Phys. Rev. Lett.* **109** 235305
- [56] Lieb E H and Liniger W 1963 *Phys. Rev.* **130** 1605
- [57] Lieb E H 1963 *Phys. Rev.* **130** 1616
- [58] Fetter A L and Walecka J D 2012 *Quantum Theory of Many-Particle Systems* (North Chelmsford, MA: Courier Corporation)
- [59] Kanamoto R, Carr L D and Ueda M 2008 *Phys. Rev. Lett.* **100** 060401
- [60] Kanamoto R, Carr L D and Ueda M 2010 *Phys. Rev. A* **81** 023625
- [61] Syrwid A and Sacha K 2015 *Phys. Rev. A* **92** 032110
- [62] Syrwid A, Brewczyk M, Gajda M and Sacha K 2016 *Phys. Rev. A* **94** 023623
- [63] Oldziejewski R, Górecki W, Pawłowski K and Rzażewski K in preparation
- [64] Oldziejewski R, Górecki W, Pawłowski K and Rzażewski K 2018 *Phys. Rev. A* **97** 063617
- [65] Somewhat analogous transition was considered in: Fialko O, Delattre M-C, Brand J and Kolovsky A R 2012 *Phys. Rev. Lett.* **108** 250402
- [66] Mottelson B 1999 *Phys. Rev. Lett.* **83** 2695
- [67] Hamamoto I and Mottelson B 1990 *Nucl. Phys. A* **507** 65
- [68] Abramowitz M and Stegun I A 1964 *Handbook of Mathematical Functions: with Formulas, Graphs, and Mathematical Tables* vol 55 (North Chelmsford, MA: Courier Corporation)
- [69] Doganov R A, Klaiman S, Alon O E, Streltsov A I and Cederbaum L S 2013 *Phys. Rev. A* **87** 033631
- [70] Von Stecher J, Greene C H and Blume D 2008 *Phys. Rev. A* **77** 043619
- [71] Blume D 2012 *Rep. Prog. Phys.* **75** 046401
- [72] Christensson J, Forssén C, Åberg S and Reimann S 2009 *Phys. Rev. A* **79** 012707
- [73] Klaiman S, Lode A U, Streltsov A I, Cederbaum L S and Alon O E 2014 *Phys. Rev. A* **90** 043620
- [74] Imran M and Ahsan M 2015 *Adv. Sci. Lett.* **21** 2764
- [75] Beinke R, Klaiman S, Cederbaum L S, Streltsov A I and Alon O E 2015 *Phys. Rev. A* **92** 043627
- [76] Bolsinger V, Krönke S and Schmelcher P 2017 *J. Phys. B: At. Mol. Opt. Phys.* **50** 034003
- [77] Bolsinger V, Krönke S and Schmelcher P 2017 *Phys. Rev. A* **96** 013618

- [78] Jeszenszki P, Cherny A Y and Brand J 2018 *Phys. Rev. A* **97** 042708
- [79] Lanczos C 1950 *J. Res. Natl. Bur. Stand.* **45** 2133
- [80] Kotochigova S 2014 *Rep. Prog. Phys.* **77** 093901
- [81] Castin Y and Dum R 1998 *Phys. Rev. A* **57** 3008
- [82] Leggett A J 2001 *Rev. Mod. Phys.* **73** 307
- [83] Fölling S, Gerbier F, Widera A, Mandel O, Gericke T and Bloch I 2005 *Nature* **434** 481
- [84] Schellekens M, Hoppeler R, Perrin A, Gomes J V, Boiron D, Aspect A and Westbrook C I 2005 *Science* **310** 648
- [85] Esteve J, Trebbia J-B, Schumm T, Aspect A, Westbrook C I and Bouchoule I 2006 *Phys. Rev. Lett.* **96** 130403
- [86] Jeltes T *et al* 2007 *Nature* **445** 402
- [87] Dür W, Vidal G and Cirac J I 2000 *Phys. Rev. A* **62** 062314
- [88] Pezzé L and Smerzi A 2009 *Phys. Rev. Lett.* **102** 100401
- [89] Haas F, Volz J, Gehr R, Reichel J and Estève J 2014 *Science* **344** 180
- [90] Bisset R N, Baillie D and Blakie P B 2011 *Phys. Rev. A* **83** 061602
- [91] Bisset R N, Baillie D and Blakie P B 2012 *Phys. Rev. A* **86** 033609
- [92] Ticknor C 2012 *Phys. Rev. A* **85** 033629